Structure formation in yttrium aluminum garnet (YAG) fibers

ARTICLE *in* JOURNAL OF THE EUROPEAN CERAMIC SOCIETY · MAY 2014

Impact Factor: 2.95 · DOI: 10.1016/j.jeurceramsoc.2013.10.036

Available online at www.sciencedirect.com

ScienceDirect

Journal of the European Ceramic Society 34 (2014) 1321–1328

www.elsevier.com/locate/jeurceramsoc

Structure formation in yttrium aluminum garnet (YAG) fibers

Stephanie Pfeifer[a,b], Markus Bischoff[c], Rainer Niewa[c], Bernd Clauß[b,*], Michael R. Buchmeiser[a,b,**]

[a] *Institute of Polymer Chemistry, University of Stuttgart, Pfaffenwaldring 55, D-70569 Stuttgart, Germany*
[b] *Institute of Textile Chemistry and Chemical Fibers, Körschtalstraße 26, D-73770 Denkendorf, Germany*
[c] *Institute of Inorganic Chemistry, University of Stuttgart, Pfaffenwaldring 55, D-70569 Stuttgart, Germany*

Received 3 July 2013; received in revised form 25 October 2013; accepted 29 October 2013
Available online 12 December 2013

Abstract

Polycrystalline yttrium aluminum garnet (YAG, $Y_3Al_5O_{12}$) fibers were prepared from aqueous solutions of aluminum chlorohydrate and yttrium chloride. Fiber processing was accomplished via dry spinning. Poly(vinylpyrrolidone) (PVP) was used as spinning aid. Polycrystalline YAG fibers were obtained by pyrolysis of the green fibers followed by sintering at defined temperatures in air. Ceramic fibers were 9–16 μm in diameter. Differential scanning calorimetry/thermogravimetric analysis coupled with mass spectrometry (DSC/TGA-MS) showed an exothermic peak at 920 °C assigned to the crystallization of YAG and an overall ceramic yield of 38% at 1400 °C. X-ray diffraction (XRD) analysis showed that phase-pure YAG can be obtained at 1600 °C after intermediate formation of Y_2O_3 and monoclinic yttrium aluminum oxide (YAM, $Y_4Al_2O_9$) phases.

Keywords: Yttrium aluminum garnet (YAG) fiber; Phase formation; Microstructure; Ceramic fiber

1. Introduction

Oxide ceramic fibers as reinforcement for ceramic matrix composites are of enormous interest for technical applications in both aerospace and power engineering industry. They exhibit excellent properties such as high temperature and corrosion resistance as well as excellent mechanical stability. Furthermore, compared to metals, they are characterized by a relatively low density.[1] During the last decades, special efforts have been devoted to the development of oxide ceramic fibers based on corundum and mullite, which are now commercially available. The fibers are produced with small grain sizes in order to obtain high tensile strengths.[2–8] Since the creep rate of polycrystalline oxide ceramic fibers increases with decreasing grain size, the creep resistance of the commercially available ultrafine grained fibers is comparatively low. The so far developed oxide ceramic fibers do not only tend to creep under mechanical stress at temperatures exceeding 1100 °C, but are also prone to embrittlement due to grain growth. They therefore cannot satisfy the growing requirements especially in terms of chemical and mechanical stability in long-term, high temperature use in oxidizing atmospheres.[9] That is why there is a high demand on the optimization of their creep resistance and high temperature performance.

With respect to the optimization of the ceramic microstructure as well as to the improvement of creep resistance, yttrium aluminum garnet (YAG, $Y_3Al_5O_{12}$) is a promising candidate. YAG is the only thermodynamically stable yttrium aluminum oxide. It is characterized by a very high melting point of 1940 °C and known as the oxide with the highest creep resistance.[10–12] Furthermore, it is chemically inert under both reducing and oxidizing atmospheres.[10–14] For these reasons, yttrium aluminum oxide is a promising material to outperform the so far developed ceramic fibers in this area.

YAG fibers have been investigated by the 3 M Co. as well as by other research groups. 3 M Co. produced short length YAG fibers with a low tensile strength of 0.7 GPa, probably because of substantial porosity. The grain size was 0.1 μm at 1200 °C. For high-temperature applications, they postulated a

* Corresponding author. Tel.: +49 0711 9340 126.
** Corresponding author at: Institute of Polymer Chemistry, University of Stuttgart, Pfaffenwaldring 55, D-70569 Stuttgart, Germany.
Tel.: +49 0711 685 64075.
E-mail addresses: bernd.clauss@itcf-denkendorf.de (B. Clauß), michael.buchmeiser@ipoc.uni-stuttgart.de (M.R. Buchmeiser).

0955-2219/$ – see front matter © 2013 Elsevier Ltd. All rights reserved.
http://dx.doi.org/10.1016/j.jeurceramsoc.2013.10.036

maximum temperature of 1200 °C, which is about 50 °C higher than the one for Nextel™ 720 fibers.[1] King et al. prepared endless YAG filament fibers from colloidal sols of Y_2O_3 and AlO(OH) and water-soluble polymers. The structural formation of YAG proceeded via various intermediate phases such as yttrium aluminum perovskite (YAP, $YAlO_3$) and monoclinic yttrium aluminum oxide (YAM, $Y_4Al_2O_9$) below 1300 °C. Up to 1300 °C, considerable porosity was found which vanished after sintering at 1700 °C due to grain growth and densification. While the creep resistance of these fibers evaluated using the bend stress relaxation (BSR) technique[15] was good, the bend strength was only 0.522 GPa.[16] YAG fiber preparation via other precursor routes was abandoned due to higher porosity and poor sintering behavior.[17,18] Popovich et al. synthesized melt-spun YAG fibers from a mixture of crystalline and amorphous YAG powders and a thermoplastic polymer. YAG, which was synthesized from yttrium and aluminum nitrates and glycine, formed gradually with an intermediate phase (YAP) after one hour of sintering at 1000 °C. The diameter of the sintered fiber was 104 μm and the bend strength was measured as 0.577 GPa by a loop bend test.[19] Pullar et al.[20–22] reported YAG staple fibers prepared via an adapted commercial blow-spinning process[23] from sol–gel precursors (aluminum chlorohydrate "Locron L" and $Y(OH)_3$-sols prepared by different yttrium salts including yttrium chloride) using PEO as spinning aid. The phase formation of YAG is described to occur in one step after heat treatment of 800 °C for the yttrium nitrate containing precursor and 900 °C for the yttrium chloride containing precursor, respectively. However, they found yttrium chloride to be a superior precursor salt. Whereas strain estimation experiments and friability tests revealed the weakness of the YAG fibers, they succeeded in improving the results by steaming the fibers during sintering. The friability test showed that 65% of the steamed fibers heated to 1550 °C were retained. Comparing two different aluminum chlorohydrates ("Locron L", containing 160 ppm sodium, and "Chlorohydrol", sodium-free), they observed that even small amounts of sodium affect the creep resistance in YAG.[21–23] Liu et al. prepared YAG short fibers as well as YAG endless fibers from $Y(OAc)_3{\cdot}4\ H_2O$, $Al(O_2CH)_3{\cdot}3\ H_2O$ and Y- and Al-isobutyrates. Fibers were sintered at 1600 °C and had grain sizes of 1.8 μm.[24,25] Li et al. prepared YAG fibers from aqueous solutions of aluminum powder and $Y(OAc)_3{\cdot}4\ H_2O$ via a sol–gel process with PEO as spinning aid. The fibers were processed via a centrifugal spinning technique. YAG phase formation was finished at 900 °C. While grain growth occurred more rapidly with increasing sintering temperature, the tensile strength decreased continuously from 0.97 to 0.38 GPa.[26]

The so far conducted studies show that YAG fibers prepared on a laboratory scale generally do not have good tensile strengths even though the creep resistance was found to be very good. Most fibers were synthesized by expensive sol–gel processes. Although its potential as ceramic fiber material and its mechanical behavior have been investigated, the complete phase formation process in YAG fibers at least based on molecular disperse solutions of Al- and Y-chlorides has not been studied comprehensively. The aim of the present work was to study both the complex phase formation processes by X-ray diffraction (XRD) and differential scanning calorimetry/thermogravimetric analysis coupled to mass spectrometry (DSC/TGA-MS) and the corresponding microstructural evolution by scanning electron microscopy (SEM).

2. Experimental

2.1. Preparative methods

2.1.1. Synthesis of stable spinning dopes

The YAG precursor spinning dope was prepared by using basic aluminum chloride ($Al_2(OH)_5Cl{\cdot}2.5\ H_2O$) and yttrium chloride ($YCl_3{\cdot}6\ H_2O$) as raw materials. The calculated amount of $Al_2(OH)_5Cl{\cdot}2.5\ H_2O$ was used as 50 wt.% aqueous solution (Locron L, Clariant, alumina content: 23.2 wt.%). The YAG precursor solution with an Y:Al molar ratio of 3:5 was synthesized by dissolving $YCl_3{\cdot}6\ H_2O$ (Strem Chemicals, Inc., 99.9%) in pure H_2O, adding 5 wt.% of malonic acid and mixing with a 50 wt.% aqueous solution of $Al_2(OH)_5Cl{\cdot}2.5\ H_2O$. To obtain a solution suitable for fiber spinning, poly(vinylpyrrolidone) (PVP) was used as spinning aid. The solution was stirred at room temperature for 30 min and concentrated in a rotary evaporator to adjust the required viscosity for fiber spinning.

2.1.2. Spinning procedure

Fibers were both hand drawn and produced by a dry spinning technique. For hand drawn fibers, a glass rod was inserted into the viscous YAG precursor solution and withdrawn. In order to obtain defined diameters, the fibers were put on a continuously rotating godet located 1.20 m above the spinning dope. The resulting fibers were subjected to air drying on a metal frame. For dry spun fibers, the viscous YAG precursor solution was poured into a spinning vessel with a spinning pump and a spinneret with 90 holes, each having diameters of 100 μm. Pressure was applied for fiber spinning and the fibers were dried in the spinning chamber in air at 60 °C and 50 °C. Finally, the multifilament green fibers were collected on a bobbin.

2.1.3. Pyrolysis and sintering

For pyrolysis and sintering, the fibers were cut into pieces of 10–15 cm length, put on an Al_2O_3 plate and heated under tension in air to various temperatures. Heat treatment was carried out at temperatures ranging from 600 to 1700 °C with a heating rate of 2 K/min and a dwell time of 1 h at the end temperature for phase formation studies. In order to investigate the microstructural evolution, fibers were heat-treated either between 600 and 1100 °C for 10 min or stepwise with a dwell time of 10 or 30 min at 600 °C and/or 900 °C and 1000 °C. After heat treatment, fibers were allowed to cool to room temperature inside the furnace.

2.2. Characterization

Thermal analysis measurements were carried out on a DSC/TGA-MS instrument (Netzsch STA 449 *F3 Jupiter*® coupled with QMS 403 Aëolos®) at a heating rate of 10 K/min

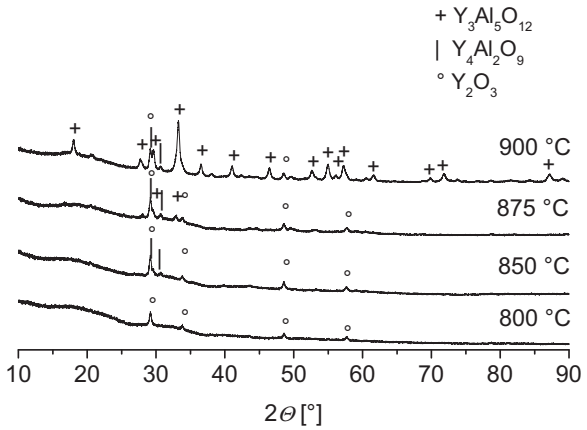

Fig. 1. XRD patterns of YAG precursor fibers heated to 800, 850, 875 and 900 °C.

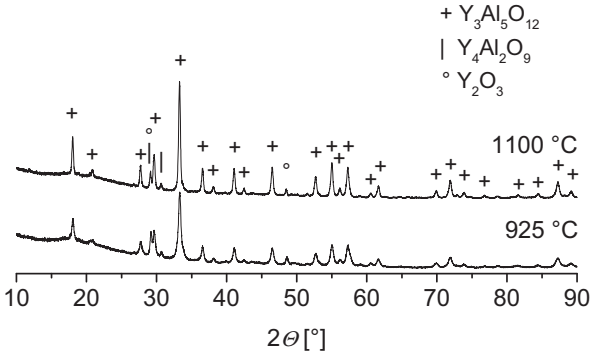

Fig. 2. XRD patterns of YAG precursor fibers heated to 925 and 1100 °C, respectively.

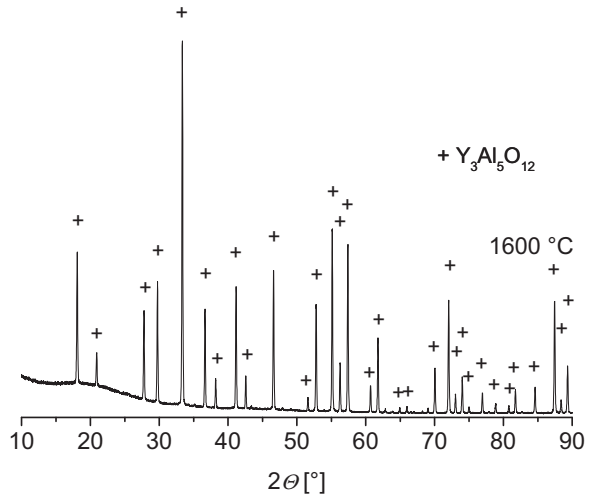

Fig. 3. XRD pattern of YAG precursor fibers heated to 1600 °C.

in synthetic air/nitrogen (gas flow 100 mL/min air/10 mL/min N_2) and a final sintering temperature of 1400 °C. For measuring samples of ground green fibers were placed in Al_2O_3 crucibles.

X-ray powder diffraction patterns of the samples treated at various temperatures were recorded on a STADI P diffractometer (STOE & Cie GmbH, Darmstadt) with a position-sensitive detector in transmission mode with Cu-$K_{\alpha 1}$-radiation in the region of $10 < 2\Theta < 90°$. XRD samples were produced by grinding YAG ceramic fibers which had been heat-treated as described above. The preparation of the sample was carried out with the aid of Scotch Magic (invisible tape).

Scanning electron microscopy and analysis of the morphology of the ceramic fiber samples were carried out on an Auriga field emission scanning electron microscope (Zeiss, Jena). For preparation, fiber samples were sputtered with platinum/palladium (layer thickness 3–5 nm).

Scanning electron microscopy and energy dispersive X-ray spectroscopy were conducted on an Auriga field emission scanning electron microscope (Zeiss, Jena) with an XMax 50 detector (Oxford Instruments). Fiber samples were sputtered with carbon for preparation (layer thickness ~ 15 nm).

3. Results and discussion

3.1. Crystallization

XRD measurements on YAG precursor fibers heated to 600 °C revealed a broad hump suggesting the presence of amorphous phases. Low intensity reflections indicate the formation of crystalline phases, however, of unknown identity. At 700 °C, Y_2O_3 started to crystallize in the space group $Ia\bar{3}$ but the crystallinity was still very low (Fig. A.1).[27] At this temperature, the above-mentioned unknown phases had almost vanished and signal intensities increased continuously upon heating to 800 °C. At this temperature, Y_2O_3 in the space group $Ia\bar{3}$ was the only crystalline phase, but few broad reflections of very low intensity may be due to a second amorphous phase (Fig. 1). At 850 °C, Y_2O_3 remained the major crystalline phase. In parallel, YAM ($Y_4Al_2O_9$) started to form.[28] At 875 °C, the major phase was still Y_2O_3 ($Ia\bar{3}$). In addition, YAM and YAG could be identified (Fig. 1).[29] In terms of mechanism of structure formation, it can be assumed that parts of Y_2O_3 reacted with amorphous γ-Al_2O_3 or AlO(OH) to form YAM and YAG as well as parts of YAM reacted with γ-Al_2O_3 or AlO(OH) to form YAG.

At 900 °C, the crystallinity increased with YAG being the main component. Y_2O_3 and YAM were detected as by-products with the amount of Y_2O_3 being slightly higher than the one of YAM. This indicates that YAM and amorphous γ-Al_2O_3 or AlO(OH) were transformed into YAG (Fig. 1).

The decrease in signal intensities of both Y_2O_3 and YAM at 925 °C suggests a further reaction of YAM and Y_2O_3 with amorphous γ-Al_2O_3 or AlO(OH) into YAG (Fig. 2). Up to 1100 °C, the amount of Y_2O_3 was higher than the one of YAM but at 1200 °C the ratio of YAM to Y_2O_3 reversed (Figs. 2 and A.1). This provides evidence that the transformation of YAM to YAG is faster than the reaction of Y_2O_3 at temperatures below 1200 °C. The intensities of the YAG signals increased and the reflections refined as the temperature was raised from 1000 to 1700 °C, which indicates continuing crystallization and enhancing crystallinity of YAG. At 1600 °C, nearly phase-pure YAG was obtained (Fig. 3). However, some traces of α-Al_2O_3 could be identified, too (Fig. A.2).[30] There are two possible explanations for the presence of small amounts of α-Al_2O_3.

Most probably, a residual amount of γ-Al_2O_3 has been converted to α-Al_2O_3. However, one cannot completely rule out some contamination coming from the α-Al_2O_3 crucibles used for the sample preparation.

To summarize, the crystallization of YAG from yttrium chloride and basic aluminum chloride occurs gradually from the amorphous precursor with the formation of intermediate phases of Y_2O_3 and YAM with increasing temperature, finally leading to the presence of single-phase YAG. The whole phase formation process is quite complicated and extends over a wide temperature range from the onset of YAG crystallization until the formation of single-phase YAG. As the temperature required to form single-phase YAG indicates the reactivity of the YAG precursors and also the level of homogeneity of the material it can be concluded that the reactivity of the YAG precursors is considerably low. However, solid state diffusion of Y^{3+} and Al^{3+} is indispensable for nucleation and growth of the YAG phase. A greater diffusion distance requires a larger diffusivity for rapid formation of single-phase YAG and therefore higher temperatures.[17] We assume that the YAG precursors build a molecular dispersed spinning solution and therefore show a high degree of homogeneity, which is preserved during fiber spinning. However, a partial segregation during heat treatment is possible, which affects the diffusion distance between reacting species. YAG starts to form at temperatures as low as 875 °C on a nano-scale, which indicates certain diffusivity. Not only local inhomogeneities in the yttria/alumina ratio but also the very slow grain growth kinetics of YAG could provide the opportunity for side reactions to YAM. Furthermore, it is possible that YAM solid state nucleation is faster than the one of YAG.[17] Single phase YAG can be obtained by sintering for 1 h at 1600 °C.

3.2. Heat treatment

Measurements by means of DSC/TGA coupled to MS allow the interpretation of the decomposition and transformation processes occurring during the heat treatment of the green fiber material and therefore represent a supplementary analyzing method. The TGA curve of the YAG precursor spinning dope shows seven mass loss steps during pyrolysis and sintering (Fig. A.3). The first mass loss of 14.4 wt.% at 144 °C corresponds to the elimination of crystal water as identified by MS and is accompanied by an endothermic peak at 142 °C in the DSC (Fig. 4). This mass loss is followed by a second endothermic event at 281 °C according to a mass loss of 13.8 wt.% at 282 °C (Figs. 4 and A.3). The endothermic peak can be assigned to several events such as to an additional loss of water and to the start of the decomposition of both malonic acid (volatilization of the fragments $CO_2^{\bullet+}$ and $CO_2H^{\bullet+}$; $m/z = 44$ and 45) and PVP (detection of $CO_2^{\bullet+}$, $m/z = 44$; Fig. 4). Also, the release of gaseous hydrochloric acid (HCl), which shows up in the MS as $Cl^{\bullet+}$ ($m/z = 35$) and $HCl^{\bullet+}$ ($m/z = 36$), from the precursor salts occurs (Fig. 5).

The third mass loss is centered at 452 °C (mass loss of 15.2 wt.%, Fig. A.3). At this temperature, not only further water evaporates from the system, but continuing oxidative decomposition of malonic acid occurs as provided by detection of the masses $m/z = 44$ ($CO_2^{\bullet+}$) and 45 ($CO_2H^{\bullet+}$), respectively. However, some further decomposition products of PVP are found in this third mass loss event supported by small amounts of typical fragments like $C_3H_3^{\bullet+}$, $C_2H_3N^{\bullet+}$, and $CO_2^{\bullet+}$, ($m/z = 39$, 41, and 44; Figs. 4 and 6). Besides, the main part of hydrochloric

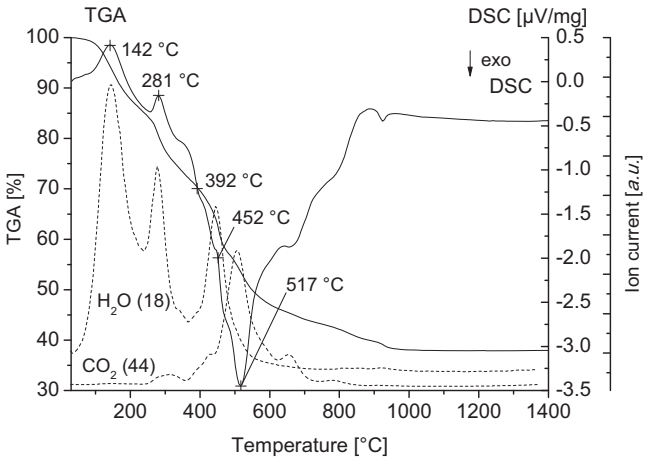

Fig. 4. DSC and TGA curves (solid lines) with the corresponding ion currents of $m/z = 18$ ($H_2O^{\bullet+}$) and 44 ($CO_2^{\bullet+}$) (dashed lines).

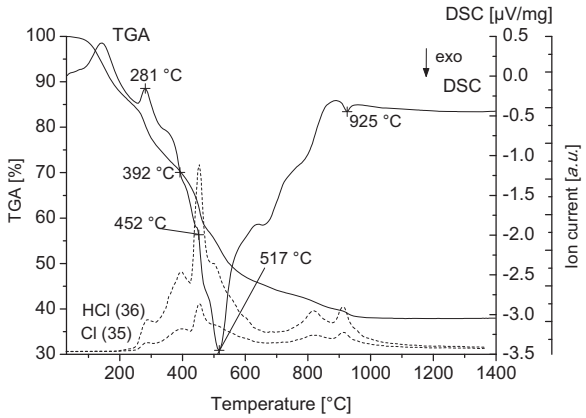

Fig. 5. DSC and TGA curves (solid lines) with the corresponding ion currents of $m/z = 35$ ($Cl^{\bullet+}$) and 36 ($HCl^{\bullet+}$) (dashed lines).

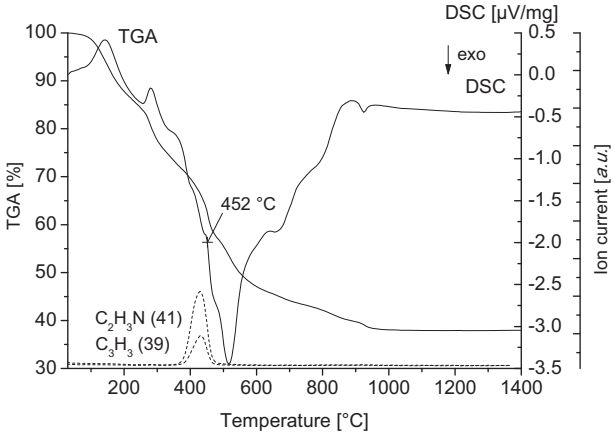

Fig. 6. DSC and TGA curves (solid lines) with the corresponding ion currents of the PVP fragments (dashed lines).

acid is also released in this mass loss step ($m/z = 35, 36$; Fig. 5). The fourth mass loss step between 487 and 640 °C (centered at 520 °C, mass loss of 10.9 wt.%; Fig. A.3) is caused by the main decomposition of the polymer (PVP), which is associated with a strongly exothermic peak at 517 °C in the DSC (Fig. 6).

Major amounts of CO_2 can be detected at this temperature by MS (Fig. 4). Furthermore, there is evidence that the release of malonic acid has not been finished since very small amounts of the fragment $m/z = 45$ are detected again. The system also loses some more gaseous hydrochloric acid during this exothermic reaction. However, even after the decomposition of the organic compounds, the mass loss is not completely finished. The sample continues to slowly decrease in weight with small thermal changes until the crystallization of YAG occurs. The weight loss between 640 and 741 °C (centered at 675 °C, mass loss of 2.3 wt.%; Fig. A.3) is associated with the final liberation of residual amounts of the decomposition products of PVP and malonic acid as indicated by very low MS ion currents of $m/z = 44$ and 45 (Fig. 4). The accompanying exothermic event can be assigned to the onset of crystallization of Y_2O_3 as indicated by the XRD pattern of the fiber, which has been heat-treated up to 700 °C (Fig. A.1). There are two more exothermic events between 741 and 1003 °C, accompanied by weight losses of 3.4 wt.% and 2 wt.%, centered at 827 °C and 927 °C, respectively, resulting in an overall mass yield of 38 wt.%. They are caused by the volatilization of gaseous hydrochloric acid, which originate from the precursors as identified by MS (Fig. 5). Furthermore, there is some CO_2 liberated during the sixth weight loss step between 741 and 883 °C, which presumably originates from the decomposition of an intermediary formed yttrium carbonate species (Figs. 4 and A.4). The DSC plots exhibit exothermic events around 828 and 920 °C, which can be assigned to the onset of crystallization of YAM and YAG, respectively, as has been proved by comparison with the XRD pattern of the samples at 850 and 875 °C (Fig. 1).

According to DSC/TGA-MS analysis, the heat treatment process of YAG green fibers generally entails three different stages that are interlocked: (i) elimination of water and removal of volatile organics at low temperatures (30–487 °C); (ii) decomposition of organic compounds such as malonic acid and PVP at intermediate temperatures (371–640 °C); and (iii) volatilization of CO_2 due to the decomposition of an intermediary formed yttrium carbonate species and crystallization of the fibers at high temperatures (640–1003 °C). The three stages the heat treatment process consists of as well as the entire manufacturing process of YAG ceramic fibers are summarized in Fig. 7.

Gaseous hydrochloric acid is released over a wide temperature range, namely at 282, 452, 520, 827 and 927 °C with a major fraction being liberated at 452 °C. However, considerable amounts of chloride ions remain in the system up to the point where the crystallization of YAM and YAG occurs and are then released in course of the phase transformation. This suggests the presence of an amorphous Y-/Al-chloro-species. The discrepancy between the crystallization temperature of Y_2O_3, YAM and YAG determined by XRD and by DSC/TGA-MS data can be explained by differences in the heating schedule. The XRD samples were heat-treated at selected temperatures for one hour, which provided enough time for the individual phases to crystallize. In contrast, the DSC/TGA-MS samples were heated applying a high heating rate of 10 K/min up to 1400 °C shifting the crystallization temperatures to higher values. That is why the exothermic crystallization peak of YAG occurs at 920 °C in the DSC rather than at 875 °C as observed by XRD. Notably, this dependence of phase formation on the heating schedule was also noticed by other groups.[23,24]

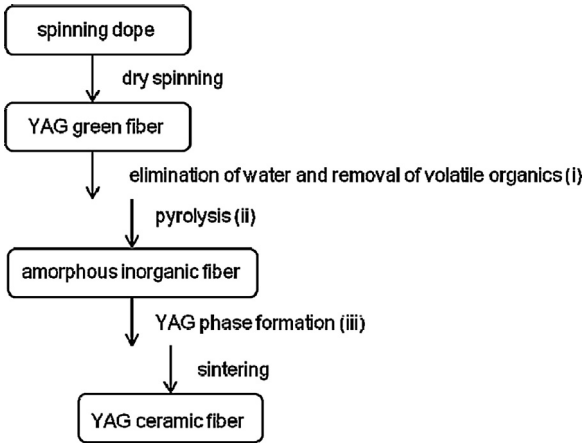

Fig. 7. Manufacturing process of YAG ceramic fibers.

3.3. Microstructure

Based on the DSC/TGA-MS data, heat treatment of the YAG green fibers was carried out stepwise. The process entailed different stages, i.e. one with a low heating rate (2 K/min) during the elimination of water and removal of organic material at low temperatures, a dwell time to allow diffusion of the gaseous cleavage products to the fiber surface and another stage that comprised higher heating rates (5 K/min) during the volatilization of chlorine at intermediate temperatures. The crystallization and densification of the fibers finally occurred at high temperatures. Fibers that were heat-treated with a heating rate of 2 K/min to 600 °C and with 5 K/min to 1000 °C, with a dwell time of 10 min each, exhibited a circular cross section with an average ceramic fiber diameter of 9 μm and mostly smooth surfaces. The microstructure was granular with a grain size well below 80 nm. The fracture surface revealed a very fine microstructure and a certain intergranular porosity on the nano-scale (Fig. 8(a–c)).

In order to determine the importance of dwell time during polymer decomposition, the crystallization of YAG and its densification, fibers were heat-treated applying a heating rate of 2 K/min to 600 °C with a longer dwell time of 30 min instead of 10 min to allow diffusion of the decomposition products to the fiber surface. Then, according to the XRD and DSC/TGA-MS results, they were heated with 5 K/min to 900 °C with an additional dwell time of 10 min during crystallization of YAG and finally sintered to 1000 °C for 30 min in order to achieve better densification. The SEM micrographs of the thus treated fibers showed spherical cross sections with an average ceramic fiber diameter of 9 μm. The microstructure exhibited no obvious improvement in terms of porosity. The fibers were still very fine grained with a grain size less than 100 nm and a

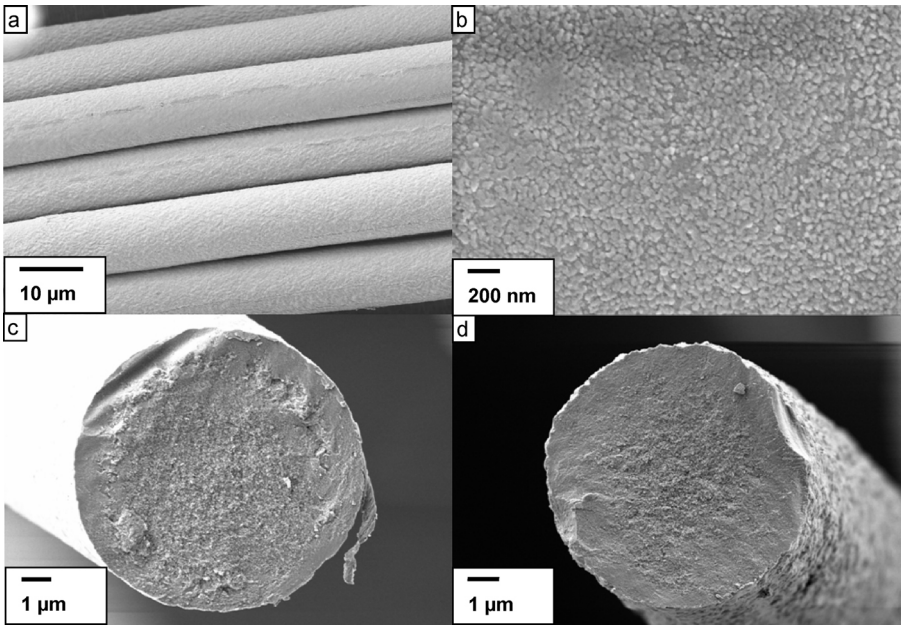

Fig. 8. SEM micrographs of the surfaces (a and b) and fracture surface (c) of dry-spun YAG fibers heated with 2 K/min to 600 °C and with 5 K/min to 1000 °C, dwell time of 10 min each; fracture surface of a dry-spun fiber heated with 2 K/min to 600 °C for 30 min, with 5 K/min to 900 °C for 10 min and then with 5 K/min to 1000 °C for 30 min (d).

porosity in the nano-range (Fig. 8(d)). As it is known from DSC/TGA-MS that elimination of water and decomposition of the polymer and malonic acid occurs gradually over a wide temperature range, it is indispensable to choose low heating rates at temperatures up to 600 °C because rapid release of water and organics can cause the fibers to bloat and crack. Also, long gas diffusion distances in case of a large fiber diameter could result in fiber damage. Obviously, heating rates were well chosen and fiber diameters were small enough. Because water and organics could diffuse out easily, crack free fibers could be obtained. However, fibers were not fully dense at 1000 °C but consisted of YAG grains smaller than 100 nm with fine intergranular porosity. The homogeneity of the fibers was confirmed by EDX mapping (Fig. A.5). The presence of porosity can be explained by the persistent release of CO_2 during the crystallization of Y_2O_3 and YAM at temperatures >600 °C. Because of the complicated crystallization and high creep resistance of YAG, the lattice diffusion rate is very low. Thus,

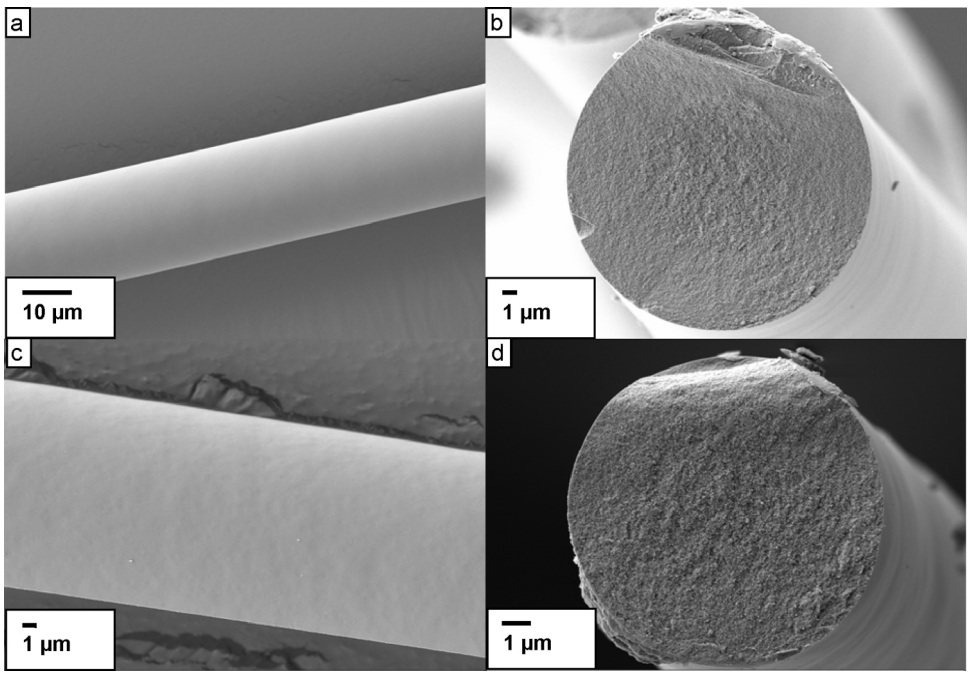

Fig. 9. SEM micrographs of the surfaces and fracture surfaces of hand drawn YAG fibers heated with 2 K/min to 600 °C for 10 min (a and b) and with 2 K/min to 900 °C for 10 min (c and d).

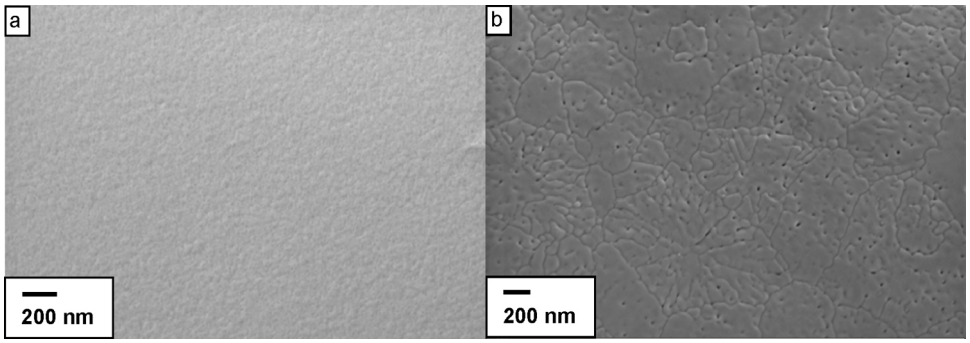

Fig. 10. SEM micrographs of the surfaces of dry spun YAG fibers heated with 2 K/min to 600 °C for 10 min (a) or with 2 K/min to 1100 °C for 10 min (b).

grain growth of YAG is extremely slow and the continuous volatilization of CO_2 could result in a certain porosity.[13] Dwell times of 10 min at 600, 900 and 1000 °C or extended dwell times of 30 min at 600 and 1000 °C did not result in improved density.

SEM micrographs of green fibers that have been heated to different temperatures revealed the evolution of the microstructure of the final YAG fibers. A low heating rate of 2 K/min was chosen to avoid any rapid evaporation of water and decomposition of organics in order to obtain smooth fiber surfaces and prevent the fibers from cracking and bloating. Therefore, YAG precursor fibers heated up to 600 °C for 10 min exhibited a smooth surface. Although it is known from XRD measurements that the crystallinity is low at 600 °C, the surface as well as the fracture surface of the heat-treated fiber already looked polycrystalline with a very fine grained microstructure and nano-scaled pores. The grain and pore sizes were far below 100 nm (Fig. 9(a and b). No differences with regards to the microstructure of the fracture surfaces were observed as the end temperature was increased in steps of 100–1100 °C (Figs. 9(c,d) and A.6).

However, the increase in crystallinity was successfully demonstrated by XRD measurements. Thus, the micrographs of the fiber surfaces still exhibited a fine microstructure, which provides evidence for the assumption that the lattice diffusion in YAG and thus the grain growth of YAG occurs very slowly. In contrast to the fine microstructure on the surface of fibers heated to 600 °C, higher end temperatures, typically 1100 °C, resulted in a grain growth at the fiber surface whereas the grains in the interior tended to retain their small grain sizes (Fig. 10). In order to obtain fully dense and defect-free polycrystalline YAG fibers, the experimental procedure has to be adapted to the results of XRD and DSC/TGA-MS measurements as described above. Notably, the microstructure of the YAG fibers presented in this publication is superior to the microstructure of the unsteamed YAG fibers produced by Pullar et al.[23] despite the fact that higher processing temperatures were applied.

4. Conclusions

Polycrystalline YAG fibers were prepared from aqueous solutions of aluminum chlorohydrate and yttrium chloride by a solution process. The start of YAG phase formation in the fibers was found to occur at 875 °C after the crystallization of intermediate phases of Y_2O_3 and YAM. Single phase YAG was found to exist at $T \geq 1350$ °C with an overall ceramic yield of 38%. The pyrolysis and sintering behavior of the YAG precursor fibers was observed to entail different stages, i.e. the elimination of fugitive compounds, decomposition of organics, crystallization and densification, resulting in gradual weight loss and detection of cleavage products. The effects of heat treatment on the microstructure of the fibers were investigated in this study, too. These results demonstrated that the heating schedule is of utmost importance for the final microstructure and chemical composition of YAG fibers. In order to obtain fully dense and defect-free polycrystalline YAG fibers, the experimental procedure has to be adapted to the results of XRD and DSC/TGA-MS measurements as described in this study.

Appendix A. Supplementary data

Supplementary data associated with this article can be found, in the online version, at http://dx.doi.org/10.1016/j.jeurceramsoc.2013.10.036.

References

1. Wilson DM, Visser LR. High performance oxide fibers for metal and ceramic composites. *Composites, Part A* 2001;**32**(8):1143–53.
2. Pysher DJ, Goretta KC, Hodder RSJ, Tressler RE. Strengths of ceramic fibers at elevated temperatures. *J Am Ceram Soc* 1989;**72**(2):284–8.
3. Lavaste V, Berger MH, Bunsell AR, Besson J. Microstructure and mechanical characteristics of alpha-alumina-based fibres. *J Mater Sci* 1995;**30**(17):4215–25.
4. Lavaste V, Besson J, Berger M-H, Bunsell AR. Elastic and creep properties of alumina-based single fibers. *J Am Ceram Soc* 1995;**78**(11):3081–7.
5. Deléglise F, Berger MH, Jeulin D, Bunsell AR. Microstructural stability and room temperature mechanical properties of the Nextel 720 fibre. *J Eur Ceram Soc* 2001;**21**(5):569–80.
6. Deléglise F, Berger MH, Bunsell AR. Microstructural evolution under load and high temperature deformation mechanisms of a mullite/alumina fibre. *J Eur Ceram Soc* 2002;**22**(9–10):1501–12.
7. Clauss B, Schawaller D. Modern aspects of ceramic fiber development. *Adv Sci Technol* 2006;**50**(1):1–8.
8. Bunsell AR, Berger MH. Fine diameter ceramic fibres. *J Eur Ceram Soc* 2000;**20**(13):2249–60.
9. Clauss B. Fibers for ceramic matrix composites. In: Krenkel W, editor. *Ceramic matrix composites*. Weinheim: Wiley-VCH; 2008. p. 1–21.
10. Corman GS. Creep of yttrium aluminium garnet single crystals. *J Mater Sci Lett* 1993;**12**(6):379–82.
11. Corman GS. High-temperature creep of some single crystal oxides. *Ceram Eng Sci Proc* 1991;**12**(9–10):1745–66.

12. Karato S, Wang Z, Fujino K. High-temperature creep of yttrium-aluminium garnet single crystals. *J Mater Sci* 1994;**29**(24):6458–62.
13. Parthasarathy TA, Mah T-I, Keller KA. Creep mechanism of polycrystalline yttrium aluminum garnet. *J Am Ceram Soc* 1992;**75**(7):1756–9.
14. Hillig WB. A methodology for estimating the mechanical properties of oxides at high temperatures. *J Am Ceram Soc* 1993;**76**(1):129–38.
15. Morscher GN, DiCarlo JA. A simple test for thermomechanical evaluation of ceramic fibers. *J Am Ceram Soc* 1992;**75**(1):136–40.
16. King BH, Halloran JW. Polycrystalline yttrium aluminum garnet fibers from colloidal sols. *J Am Ceram Soc* 1995;**78**(8):2141–8.
17. King BH, Liu Y, Baskaran S, Laine RM, Halloran JW. Yttrium aluminate ceramic fibers via pre-ceramic polymer and sol–gel routes. *Part Sci Technol* 1992;**10**(3–4):121–32.
18. King BH, Liu Y, Laine RM, Halloran JW. Fabrication of yttrium aluminate fibers. *Ceram Eng Sci Proc* 1993;**14**(7–8):639–50.
19. Popovich D, Lombardi JL, King BH. Fabrication and mechanical properties of polymer melt spun yttrium aluminum garnet (YAG) fiber. *Ceram Eng Sci Proc* 1997;**18**(3):65–72.
20. Morton MJ, Birchall JD, Cassidy JE. UK Patent 1360200, 1974.
21. Pullar R, Taylor M, Bhattacharya A. Effect of sodium on the creep resistance of yttrium aluminium garnet (YAG) fibres. *J Eur Ceram Soc* 2006;**26**(9):1577–83.
22. Pullar RC, Taylor MD, Bhattacharya AK. The manufacture of yttrium aluminium garnet (YAG) fibres by blow spinning from a sol–gel precursor. *J Eur Ceram Soc* 1998;**18**(12):1759–64.
23. Pullar RC, Taylor MD, Bhattacharya AK. The sintering behaviour, mechanical properties and creep resistance of aligned polycrystalline yttrium aluminium garnet (YAG) fibres, produced from an aqueous sol–gel precursor. *J Eur Ceram Soc* 1999;**19**(9):1747–58.
24. Liu Y, Zhang Z-F, Halloran JW, Laine RM. Yttrium aluminum garnet fibers from metalloorganic precursors. *J Am Ceram Soc* 1998;**81**(3):629–45.
25. Liu Y, Zhang Z-F, King BH, Halloran JW, Laine RM. Synthesis of yttrium aluminum garnet from yttrium and aluminum isobutyrate precursors. *J Am Ceram Soc* 1996;**79**(2):385–94.
26. Li C, Zhang Y, Gong H, Zhang J, Nie L. Preparation, microstructure and properties of yttrium aluminum garnet fibers prepared by sol–gel method. *Mater Chem Phys* 2009;**113**(1):31–5.
27. Bonnet M, Delapalme A. Redetermination of the scattering length of yttrium. *Acta Crystallogr* 1975;**A31**:264–5.
28. Lehmann MS, Christensen AN, Fjellvag H, Feidenhans'l R, Nielsen M. Structure determination by use of pattern decomposition and the rietveld method on synchroton X-ray and neutron powder data; the structures of $Al_2Y_4O_9$ and I_2O_4. *J Appl Crystallogr* 1987;**20**:123–9.
29. Euler F, Bruce JA. Oxygen coordinates of compounds with garnet structure. *Acta Crystallogr* 1965;**19**:971–8.
30. Ishizawa N, Miyata T, Minato I, Marumo F, Iwai S. A structural investigation of alpha-Al_2O_3 at 2170 K. *Acta Crystallogr* 1980;**B36**:228–30.